Biophysical Reviews (2025) 17:419–434
https://doi.org/10.1007/s12551-025-01283-0

REVIEW

The brightness of lectins conjugated to quantum dots

João V. A. Lima[1] · Weslley F. Oliveira[1] · Abdênego R. Silva[2] · Francisco P. T. Melo[1] · Martha S. Ribeiro[2] · Paulo E. Cabral Filho[1] · Adriana Fontes[1]

Received: 3 December 2024 / Accepted: 2 February 2025 / Published online: 13 February 2025

Abstract

One of the main focuses of glycobiology is investigating the synthesis and modification of carbohydrates in biological systems, due to their involvement in various processes such as cell recognition, differentiation, and immune response. Since the study of these glycans contributes to the understanding of complex biological functions, these biochemical compounds can be analyzed using lectins, which are ubiquitous proteins in nature capable of specifically recognizing carbohydrates. In addition, lectin-carbohydrate interaction can be visualized by conjugating these proteins with quantum dots (QDs), which are fluorescent nanoprobes with advantageous properties, including photostability and size-tunable emission. QDs also possess chemically active surfaces that enable the attachment of biomolecules, such as lectins. In this review, we provide detailed reports of studies involving QD-lectin conjugates conducted by the Biomedical Nanotechnology Group at the Federal University of Pernambuco (UFPE/Brazil) and its collaborators. An integrated perspective on the use of QD-lectin conjugates to study saccharides in a range of biological systems, from bacteria and fungi to red blood cells and cancer tissues, is also presented. We hope this comprehensive review inspires further studies exploring the brightness of lectins upon conjugation with QDs to unravel glycobiological processes.

Keywords Biological systems · Carbohydrate · Fluorescence · Nanocrystal

Introduction

Carbohydrates represent the third key component of the molecular alphabet of life, coming after nucleotides and amino acids (Kaltner et al. 2019). In the cells of mammals and microorganisms, oligosaccharides are typically bound to non-carbohydrate molecules (such as lipids or proteins) to form glycoconjugates. Free oligosaccharides, however, are found in plants and serve various functions, including the transport of monosaccharides through disaccharides, regulatory activities, and energy storage (Hanau et al. 2020). In addition, there are structural polysaccharides present on the cell wall, such as those of fungi and plants. Complex carbohydrates are also found in animal tissues as components of the extracellular matrix and can be stored intracellularly for energy (Fernandes and Coimbra 2023).

Moreover, changes in the glycosylation profile can alter the architecture of carbohydrates in different biological systems contributing, for example, to the metastasis of tumor cells and increasing the pathogenicity of microorganisms by enhancing their ability to evade the immune system (Lin et al. 2020; Bindeman and Fingleton 2022). Thus, unraveling the glycan composition of cells and tissues is relevant for understanding various pathologies and can provide diagnostic and therapeutic targets for a range of disorders. To elucidate the glycome of these biological systems, lectins can serve as valuable tools.

Lectins are ubiquitous proteins in nature and are characterized by having at least one carbohydrate recognition domain (CRD), which can recognize and reversibly bind

João V. A. Lima, Weslley F. Oliveira, Abdênego R. Silva, Francisco P. T. Melo, Martha S. Ribeiro, Paulo E. Cabral Filho, and Adriana Fontes contributed equally to this manuscript.

✉ Paulo E. Cabral Filho
paulo.euzebio@ufpe.br

✉ Adriana Fontes
adriana.fontes@ufpe.br

[1] Departamento de Biofísica e Radiobiologia, CB, UFPE, Universidade Federal de Pernambuco, Av. Prof. Moraes Rego, S/N, Recife, PE 50670-901, Brazil

[2] Centro de Lasers e Aplicações, Instituto de Pesquisas Energéticas e Nucleares (IPEN-CNEN), São Paulo, SP 05508-000, Brazil

to saccharides through non-covalent interactions (Tobola and Wiltschi 2022). These proteins have a wide range of biotechnological applications. For example, their ability to recognize and activate signaling pathways can be useful to exert modulatory effects in hosts or induce apoptosis in tumor cells. Furthermore, their substrate specificity, without triggering any biological effect, makes lectins helpful in immobilization techniques for purifying carbohydrates or recognizing samples in glycobiological studies. Additionally, they can serve as valuable tools in diagnosis and therapy, particularly in the context of glycosylation changes (Chettri et al. 2021). One mechanism for "visualizing" lectin recognition or understanding its action in biological systems is by conjugating these biomolecules with fluorescent compounds, such as quantum dots (QDs) (Oliveira et al. 2022).

QDs are fluorescent semiconductor nanocrystals (NCs) with diameters typically between 2 and 10 nm and have been gaining prominence in biotechnology research (Rathee et al. 2025). These NCs have unique optical and physicochemical properties, such as size-tunable emission, photostability, and active surface for conjugation with other nanoparticles (NPs) or biomolecules, for example, lectins (Yao et al. 2017; Pereira et al. 2019). These remarkable optical properties of QDs enable them to be applied in different areas, from solar cells and light-emitting devices to novel biological probes. In recognition of their contributions to the development of these nanotools, the 2023 Nobel Prize in Chemistry was awarded to A. I. Ekimov, L. E. Brus, and M. G. Bawendi, who were responsible for the discovery and synthesis of QDs.

In this review, we highlight the research activities of the Biomedical Nanotechnology Group at the Federal University of Pernambuco (UFPE/Brazil) and its collaborators, who have, for over a decade, developed conjugates composed of lectins with different specificities and carboxylated QDs to study carbohydrate profiles in various biological systems, including microorganisms, mammalian cells, and tissues. For this purpose, we have used not only lectins purified from plants typical of the Caatinga—an exclusively Brazilian biome—but also commercial and recombinant human lectins. We hope this review will inspire and guide the application of QD-lectin conjugates in future studies within the field of glycobiology.

Key concepts of lectins and quantum dots

Lectins

Lectins are a diverse group of proteins, each characterized by at least one non-catalytic domain, that specifically and reversibly recognizes and binds to monosaccharides, oligosaccharides, or glycoconjugates via the CRD, without altering the structural integrity of the carbohydrate moieties. The heterogeneity of this group of proteins, in terms of molecular structures, biochemical properties, and biophysical characteristics, can influence their biological functions (Ahmmed et al. 2022; Tsaneva and Van Damme 2020). Some lectins, for example, exhibit hemagglutination activity (HA), that is, lectin molecules interact with glycidic portions on the red blood cell (RBC) surfaces, interconnecting them and forming a network. Therefore, HA can be used to evaluate the affinity and functionality of lectins. To analyze the affinity, carbohydrates or glycoproteins are incubated with the lectin at different concentrations prior to the HA assay. The addition of carbohydrates or glycoproteins that bind to the lectins can inhibit HA by occupying the CRDs before the lectins interact with RBCs. Yet, the saccharide that promoted inhibition at the lower concentration reveals the greater specificity of the lectin (Silva et al. 2021b).

Lectin-carbohydrate recognition is primarily driven by hydrogen bonds, which enable specific recognition, while van der Waals forces and hydrophobic interactions contribute to stabilizing the binding. Aromatic stacking (between carbohydrate rings and aromatic amino acids) and electrostatic interactions (such as between arginine and sialic acid) further enhance the interaction. In addition, metal ion coordination and solvent effects can play roles: metal ions stabilize the binding site and solvation increases interaction strength by reducing water interference (Oliveira et al. 2022).

Since saccharides are not arranged in isolation on the cell surface, the presence of multiple CRDs (multivalency) on a single lectin molecule provides additional binding sites. This enables lectins to bind to multiple carbohydrate residues, thereby increasing their overall affinity for the targets (Tobola and Wiltschi 2022). Moreover, lectins exhibit a much higher affinity for carbohydrate arrangements—approximately 1000 times greater—than for monosaccharides, a phenomenon known as the cluster effect (Reynolds and Pérez 2011). Together, these characteristics enable lectins to specifically and strongly bind to glycostructures, thereby facilitating their biological functions (Tsaneva and Van Damme 2020).

Lectins are widely distributed across various biological sources, enabling their isolation and purification from animals, marine organisms, microorganisms, insects, viruses, and plants (Martínez-Alarcón et al. 2018; Mishra et al. 2019; Ahmmed et al. 2022). Plant-derived lectins, in particular, offer significant advantages due to the abundance and accessibility of biological materials such as roots, bark, rhizomes, leaves, flowers, fruits, and seeds. These proteins, predominantly isolated through chromatographic methods, are promising candidates for diverse applications, including biosensing, diagnostic assays, and antimicrobial/anticancer

therapeutical strategies (De Coninck and Van Damme 2021; Tsaneva and Van Damme 2020).

Concanavalin A (ConA), isolated from the seeds of jack bean (*Canavalia ensiformis*), was the first lectin for which the complete amino acid sequence and three-dimensional structure were determined. ConA specifically binds to structures containing terminal mannose and glucose residues and has an affinity for the methyl-α-D-mannopyranoside monosaccharide. This lectin consists of four identical monomers of about 25 kDa each. The isoelectric point (pI) of ConA, i.e., the pH at which the molecule is electrically neutral, typically ranges from 5.4 to 5.8 (Cunningham et al. 1975; Cavada et al. 2019).

Cratylia mollis, a legume native to Northeast Brazil, is part of the Leguminosae family and the Diocleinae subtribe, the same subtribe as ConA lectin. From the seeds of *Cratylia mollis*, four different molecular forms of lectins, named isoforms or isolectins, were isolated: Cramoll 1, Cramoll 2, Cramoll 3, and Cramoll 4. Isoforms 1, 2, and 4 are specific for glucose/mannose, while Cramoll 3 is a galactose-recognizing. The preparation containing the isoforms 1 and 4, named Cramoll 1,4 (commonly referred to simply as Cramoll) has been presenting different biological properties that make it suitable for biotechnological uses. This lectin has about 50 kDa and pI ranging from 8.5 to 8.6 (Pessoa et al. 2023; Correia and Coelho 1995).

From the seeds of *Ulex europaeus*, it is also possible to isolate the *Ulex europaeus* agglutinin I lectin (UEA-I). This lectin has approximately 63 kDa, consists of two subunits, and has a pI between 4.5 and 5.1. UEA-I specifically binds to L-fucose residues, commonly found on the surface of various glycoproteins and glycolipids (Gomez et al. 1995).

Another plant lectin of significance in biomedical applications is SteLL, isolated from the leaves of *Schinus terebinthifolia*. This lectin has about 14 kDa and a pI of 5.7, with a preference for binding chitin and glycoproteins (Silva et al. 2021a). Additionally, *Punica granatum* sarcotesta contains a lectin known as PgTeL, which has approximately 26 kDa and a pI of 6.5, exhibiting the same affinity as SteLL. BmoLL is also a plant lectin (Silva et al. 2021a), which is isolated from the leaves of *Bauhinia monandra* and has an affinity for galactose. BmoLL is composed of a glycosylated polypeptide chain of 33 kDa and a non-glycosylated polypeptide chain of 26 kDa (Coelho and Silva 2000). To our knowledge, the pI of BmoLL has not been reported yet.

Human-derived lectins also hold great potential as endogenous molecules for studies in glycobiology. However, their isolation and purification are limited by factors such as protein availability and ethical considerations. Consequently, recombinant protein production technologies are becoming increasingly important and widely adopted in this field (Martínez-Alarcón et al. 2018). In this context, a recombinant human mannose-binding lectin (rhMBL) can be a promising tool for glycobiological studies. The rhMBL used herein is constituted of oligomers with a molecular mass > 200 kDa and a pI ranging from 5.7 to 5.9. Native MBL is a plasma glycoprotein that plays a crucial role in the innate immune system, providing protection against infections (Lima et al. 2022). MBL is a C-type lectin with an affinity for mannose, L-fucose, *N*-acetyl-D-glucosamine (GlcNAc), and *N*-acetylmannosamine (ManNAc). This binding is enhanced by the presence of calcium ions, which stabilize the coordination bonds between the CRDs and the 3- and 4-hydroxyl groups of saccharides (Turner 2003; Lima et al. 2022).

Understanding the biophysical properties of lectins, including their size, charge, affinity, and structural characteristics, is important for advancing the development of applications in the biomedical field. When lectins are conjugated to QDs, it is possible to generate highly efficient sensing tools for detecting glycobiological patterns, offering valuable insights into cellular processes and disease mechanisms.

Quantum dots

As a class of semiconductors, QDs are fluorescent NCs characterized by a valence band (VB) and a conduction band (CB), which are separated by an energy band gap (E_g), usually lower than 3 eV (Sanmartín-Matalobos et al. 2022). Fluorescence generation of QDs begins with the excitation of electrons (e^-) from the VB to the CB. This transition occurs upon absorption of photons with an energy greater than or equivalent to that of E_g. When e^- move to the CB, they leave holes (h^+) in the VB. The resulting e^--h^+ pairs interact through coulomb force and are called excitons. As excited e^- return to the VB, excitonic recombination occurs, and fluorescence is emitted (Gidwani et al. 2021).

Each bulk semiconductor material has its own E_g and exciton Bohr radius (a_B, the e^--h^+ pair distance) (Ramalingam et al. 2020). Nevertheless, this is not the case in QDs, where e^--h^+ pairs are confined in all three dimensions to distances smaller than a_B. As a result, the size of the QDs and the width of the E_g are inversely proportional. Therefore, QDs exhibit size-tunable emission, with larger ones emitting fluorescence at longer wavelengths, and smaller ones emitting at shorter wavelengths (Fig. 1). This property has made QDs attractive across various fields, driving a broad range of studies in areas such as optoelectronics, environmental monitoring, and biomedicine, among others (Agarwal et al. 2023; Li et al. 2023; Freire et al. 2024). It is worth noting that an NP can be considered a QD only when its radius is smaller than a_B. Typically, QDs have diameters from 2 to 10 nm (Sahu and Kumar 2022).

In addition to size-tunable emission, QDs possess other advantageous optical properties (Fig. 1): (i) a broad absorption spectrum, which enables QDs of different sizes to be excited by a single light source; (ii) a narrow and

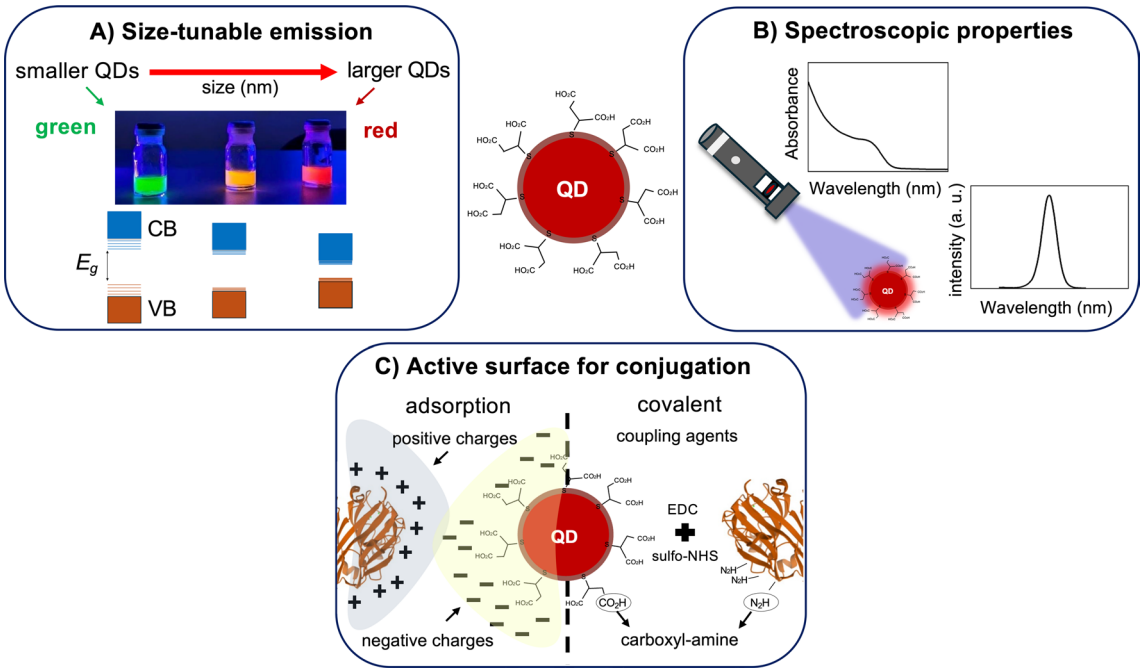

Fig. 1 Illustration of the unique physicochemical properties of quantum dots (QDs). **A** Schematic representation of the quantum confinement effect, showing the size-tunable emission of QDs. **B** Typical absorption and emission profiles of water-dispersed QDs. **C** Schematic representation of conjugation strategies (adsorption by electrostatic interaction and carboxyl-amine covalent coupling) provided by the active surface of QDs. E_g, energy band gap; CB, conduction band; VB, valence band; EDC, 1-ethyl-3-(3-dimethylaminopropyl) carbodiimide hydrochloride; sulfo-NHS, *N*-hydroxysulfosuccinimide sodium salt

symmetrical emission spectrum, which allows the development of studies using these NCs in multiplex detection assays or Föster resonance energy transfer (FRET) studies; (iii) resistance to photobleaching, which makes QDs easier to handle and suitable for long-term dynamics investigations. Moreover, QDs also have active surfaces for conjugations with molecules, such as lectins, or other nanostructures (Bilan et al. 2017; Panniello et al. 2021; Herrera-Ochoa et al. 2022; Hooper et al. 2022; Agarwal et al. 2023). With the advancement of QD applications in the life sciences, various strategies have been developed to conjugate them with a variety of compounds (Pereira et al. 2019).

One of the simplest ways to conjugate QDs is adsorption interaction involving, for instance, electrostatic forces. QDs with a negative surface charge can bind to positively charged regions of molecules, and the reverse is also possible. For this type of conjugation, controlling the pH is important to ensure the presence of opposite charges. In addition to electrostatic forces, conjugation by adsorption can be mediated by other interactions, such as van der Waals forces, hydrogen bonds, and π-π interactions (Han et al. 2014; Pereira et al. 2019).

The charge of the QDs is determined by their surface chemistry, which is typically conferred by the stabilizing agents used to keep the NCs in suspension in aqueous media. For example, carboxylated molecules, like mercaptosuccinic acid (MSA), confer negative surface charges, while amino compounds, like cysteamine, promote positive surface charges (Vo et al. 2016; Ramírez-Herrera et al. 2019). Moreover, QDs are core-shell structures. This means that these NCs typically have a core composed of a binary combination of chemical elements from groups IIB-VIA, IIIA-VA, or IVA-VIA of the earlier periodic table representation. The core is surrounded by a shell, usually made of a semiconductor with a higher E_g than the core. CdSe/ZnS, CdSe/CdS, ZnSe/ZnS, and CdTe/CdS are some examples of binary QDs (Sowers et al. 2016; Park et al. 2020; Da Costa et al. 2024; Ji Back et al. 2024; Vasudevan et al. 2021). In addition, ternary and quaternary QDs, such as AgInSe/ZnS and CdSeTeS/ZnS, respectively, have also been more recently developed (Aladesuyi et al. 2022; Adegoke et al. 2015).

The core (composition and size) determines the maximum emission wavelength of QDs, as it is associated with the quantum confinement properties and the E_g. The shell passivates the surface defects (dangling bonds) of the core, improving the emission efficiency by reducing electronic traps that contribute to non-radiative pathways. In some types of QDs, as in those prepared in aqueous media, the stabilizing agent contributes to the formation of the shell (Sahu and Kumar 2022). Additionally, these molecules also play an important role in the functionalization of QDs. The functionalizing agent can be used not only to conjugate the

QDs through adsorption interaction but also via covalent binding (Pereira et al. 2019). For the covalent approach, the functionalizing agent usually needs to be activated by specific coupling agents. For instance, carboxylic groups of QDs can be activated by the coupling agents: 1-ethyl-3-(3-dimethylaminopropyl) carbodiimide hydrochloride (EDC) alone or in combination with *N*-hydroxysulfosuccinimide sodium salt (sulfo-NHS) to react with amine groups of the molecules, or vice versa. *N*-hydroxysuccinimide (NHS) can also be used in place of sulfo-NHS. It is important to note that the pH of the suspension should be adjusted to around 5.5 before adding the coupling agents, as they have greater activity under acidic conditions (Foubert et al. 2016). It should also be noted that if carboxyl groups from QDs are activated for conjugation, they have to be blocked before biological applications to prevent non-specific interactions. This can be achieved using amino compounds, such as 2-amino-2-(hydroxymethyl)−1,3-propanediol (TRIS-base) (Cabral Filho et al. 2018). The conjugation strategies based on adsorption (electrostatic interaction) and covalent coupling (carboxyl-amine) are summarized in Fig. 1.

To assess whether there have been changes in the optical properties of QDs after conjugation, absorption and emission spectroscopies can be used. These techniques can also provide an indication of changes to the QD surface upon conjugation, but further characterization is necessary to confirm the QD-compound interaction.

Fluorescence correlation spectroscopy (FCS), for example, is a technique in which the diffusion times of nanosystems are measured and used to determine their hydrodynamic diameters. When a biomolecule, such as a lectin, is conjugated to the surface of the QDs, the diffusion time and the hydrodynamic diameter of the nanosystem increase compared to non-conjugated QDs, indicating successful conjugation (De Thomaz et al. 2014).

Another effective technique for determining conjugation is the fluorescence microplate assay (FMA), particularly if biomolecules can interact with the polystyrene that constitutes the microplates (Carvalho et al. 2014). In FMA, non-conjugated QD, biomolecules alone, and the conjugates are individually added to the wells of a black polystyrene microplate. After incubation (usually performed at 37 °C), the wells are washed with phosphate-buffered saline (PBS) or saline solution 0.9% (w/v). Immediately after the washes, the FMA analysis is performed. During the washes, the non-conjugated QDs are removed because, without the biomolecules, they cannot adhere to the wells. In the wells where only biomolecules have been added, no fluorescence is observed under the conditions applied, although biomolecules adhere to the wells. On the other hand, if the conjugation is successful, an intense fluorescence emission will be observed in the wells containing the QD-biomolecules nanosystem. The intensity values of the wells can be used to calculate the relative fluorescence (*RF*, Eq. (1)). The *RF* is expressed in percentage, and *RF* values greater than 100% indicate that the conjugation was efficient.

$$RF(\%) = \frac{FLconjugate - FLcontrol}{FLcontrol} \times 100\% \quad (1)$$

where $FL_{conjugate}$ corresponds to the fluorescence intensity emitted by the conjugate while $FL_{control}$ corresponds to the average fluorescence intensity emitted by non-conjugated QDs and the biomolecule alone (Carvalho et al. 2014).

In addition to the techniques mentioned above, biological characterizations are also important to avoid false-positive and -negative results and to determine whether the conjugation does not affect the recognition properties of the biomolecules. For this purpose, saturation or inhibition tests can be carried out. In the saturation test, before adding the conjugate, the biological system is incubated with the biomolecule, saturating the targets available for recognition by the conjugate. Conversely, in the inhibition assay, the CRD of the biomolecule present in the conjugate is inhibited by a carbohydrate to which it has an affinity. The conjugate is then incubated with the biological system. In both cases, if no significant labeling is observed, the conjugate has been successfully prepared and has specificity. Furthermore, these results also suggest that the activity of the biomolecule is preserved (Carvalho et al. 2014). As mentioned in the previous subsection, the HA assay can also serve as an alternative to investigate conjugation and the maintenance of biomolecule functionality (Silva et al. 2021a).

After confirming the interaction between the QD and the biomolecule, such as lectins, the resulting conjugate can be used to study the glycocode of biological systems. This enables a deeper understanding of complex molecular mechanisms, the development of novel diagnostic methods, and the identification of potential therapeutic targets for various diseases. In this context, the next section will highlight the applications of QD-lectin conjugates developed by our research group and collaborators, based on carboxylated CdTe/CdS QDs and lectins (Table 1). When not otherwise specified, the incubation with the biological systems was performed at room temperature.

Applications of QD-lectin conjugates

Microorganisms

Glycoconjugates establish a species-specific molecular "barcode" on the surfaces of microbial cells, enabling differentiation between species (Szymanski 2022). Furthermore, the profile of carbohydrates can impact resistance to drugs and therapies. These molecules can alter the permeability of

Table 1 Applications of QD-lectin conjugates, at cellular and tissue levels, reported in this review

Lectins	Specificity	Source	Conjugation approach	Main objective
Concanavalin A (ConA)	Glucose and mannose	Seeds from *Canavalia ensiformis*	Adsorption pH 8.0	Investigation of glucose/mannose profile of normal, fibroadenoma, and invasive ductal carcinoma human breast tissues (Andrade et al. 2013)
				Preparation and characterization of QD-ConA conjugates with application in yeast cells and biofilms of *C. albicans* (Tenório et al. 2015)
Cratylia mollis lectin (Cramoll)	Glucose and mannose	Seeds from *Cratylia mollis*	Adsorption pH 7.0	Development of QD-Cramoll conjugates using yeast cells of *C. albicans* as a biological model (Cunha et al. 2018)
				Assessment of glucose/mannose profile of normal, fibroadenoma and invasive ductal carcinoma in human breast tissues (Carvalho et al. 2019)
				Analyses of the glucose/mannose content on cells walls of *C. albicans*, *C. glabrata**, and *C. parapsilosis* (Oliveira et al. 2020a)
				Evaluation of glucose/mannose content on *Aeromonas* spp. cell surface (Pessoa et al. 2023)
Ulex europaeus agglutinin I (UEA-I)	L-Fucose	Seeds from *Ulex europaeus*	Covalent Binding EDC/sulfo-NHS pH 5.5	Investigation of L-fucose profile in normal, fibroadenoma, and invasive ductal carcinoma human breast tissues (Andrade et al. 2013)
				Obtention of UEA-I-based conjugates using green-emitting QDs and evaluation of H antigen expression on red blood cell membranes from different blood groups (Cabral Filho et al. 2015)
Punica granatum lectin (PgTeL)	Chitin and glycoproteins	Sarcotesta from *Punica granatum*	Adsorption pH 8.0	Development of QD-PgTeL conjugates using *Cryptococcus neoformans* as a biological model to evaluate the efficiency and specificity of the prepared nanosystem (Silva et al. 2021a)
				Assessment of the effects of the lectin on cells and biofilm of *Pseudomonas aeruginosa* (Silva et al. 2024)
Schinus terebinthifolia lectin (SteLL)	Chitin and glycoproteins	Leaves from *Schinus terebinthifolia*	Adsorption pH 7.0	Development of QD-SteLL conjugates using *C. neoformans* as a biological model to evaluate the efficiency and specificity of the prepared nanosystem (Silva et al. 2021a)
Bauhinia monandra lectin (BmoLL)	Galactose	Leaves from *Bauhinia monandra*	Adsorption pH 8.0	Development of QD-BmoLL conjugates and investigation of exposed galactose residues on ABO red blood cells (Oliveira et al. 2020b)
rhMBL	Mannose, L-fucose, GlcNAc, and ManNAc	—-	Adsorption pH 6.0	Investigation of using conjugation strategies based on adsorption interaction and covalent coupling in the development of QD-rhMBL conjugates using yeast cells of *C. albicans* as a biological model (Lima et al. 2022)

GlcNAc, *N*-acetyl-D-glucosamine; ManNAc, *N*-acetyl-mannosamine; rhMBL, recombinant human mannose-binding lectin. *Currently named *Nakaseomyces glabrata*

antimicrobial agents, disrupt drug binding, and enhance the pathogen's ability to evade the immune system (Riu et al. 2022). In this context, QD-lectin nanoprobes can be used to unravel the molecular mechanisms involving glycostructures in microorganisms.

Fungi

Pathogenic fungi, including *Candida albicans*, *C. parapsilosis*, *Nakaseomyces glabrata* (formerly *C. glabrata*), and *Cryptococcus neoformans* are recognized by the World Health Organization (WHO) as critical and high-priority groups threat to global health due to their rising morbidity and mortality rates (WHO 2022). The cell walls of yeasts are rich in carbohydrate residues, primarily chitin, mannose, and glucose, which can be studied using QD-lectin conjugates (Utama et al. 2023).

Tenório et al. (2015) prepared a conjugate consisting of orange-emitting QDs (600 nm), with a diameter (d) of *ca.* 3 nm, and ConA lectin. This conjugation was achieved through adsorption interaction by incubating the QD suspension (at pH 8.0) with ConA (final concentration of 280 µg/mL). Following conjugation, the ConA secondary structure was maintained, as confirmed by circular dichroism analysis. The QD-ConA conjugates displayed an HA result like that of the lectin alone, indicating that its CRD and biological functions were preserved. The HA assay was performed using glutaraldehyde-treated rabbit RBCs (in this and in the following studies). No significant changes were observed in UV-Vis absorption and emission spectra of QD-ConA conjugates compared to unconjugated QDs.

Given ConA's affinity for glucose and mannose, the conjugation was evaluated using yeast cells and biofilms of *C. albicans* (Fig. 2). Cell suspensions (1×10^6 CFU/mL) were incubated with QD-ConA conjugates in a 1:1 ratio (v/v) for 1 h. For biofilms, the wells were washed with PBS to remove the culture medium and any non-adherent cells, and then replenished with 200 µL of QD-ConA conjugates, which were incubated for 1.5 h. To evaluate the specificity of the nanosystem, a lectin binding inhibition assay was performed by incubating the conjugates with methyl-α-D-mannopyranoside (0.3 mol/L) for 30 min before incubation with *C. albicans* cells.

The flow cytometry analyses demonstrated that about 93% of yeast cells were successfully labeled by the QD-ConA nanosystem. These results were further validated by confocal fluorescence microscopy, which revealed intense labeling of both yeast cells and biofilms of *C. albicans*. The labeling was effectively inhibited by methyl-α-D-mannopyranoside, which occupied the binding sites of ConA and prevented the subsequent attachment of the QD-ConA nanosystem to the fungal structures. The obtention of the QD-ConA conjugates fostered the creation and application of several other site-specific nanoprobes for glycobiological studies (Tenório et al. 2015).

Another promising lectin for use with QDs in studies related to fungal glycobiology is Cramoll. Cunha et al. (2018) prepared a QD-Cramoll nanosystem using

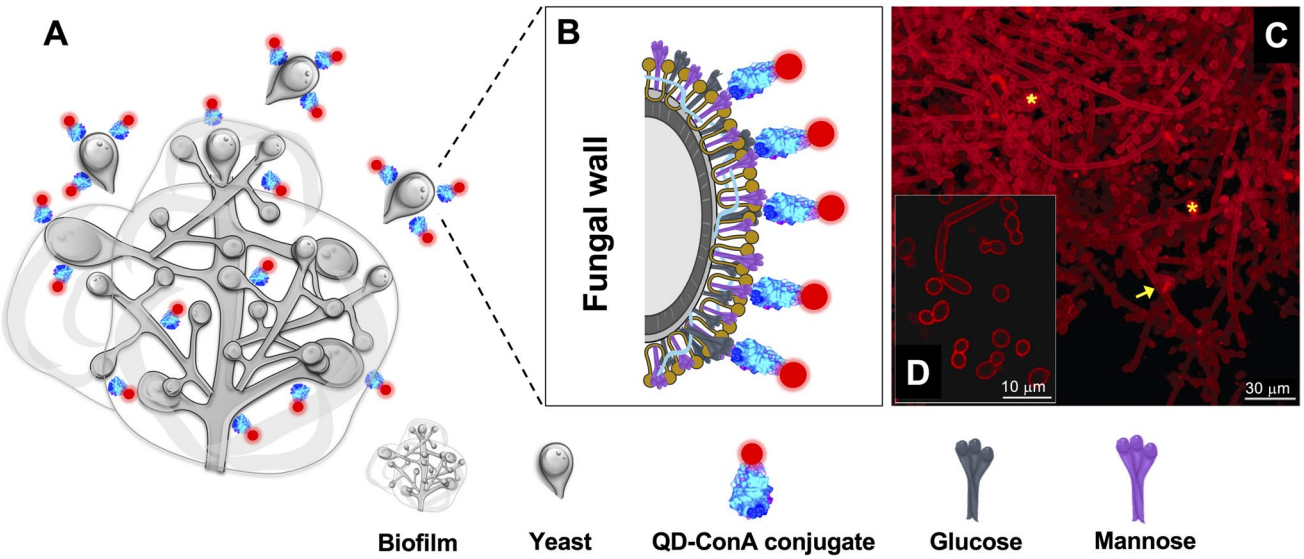

Fig. 2 **A** Schematic illustration of the interaction between glucose/mannose moieties, from *C. albicans* yeast cells and biofilms, with the QD-ConA nanotool. **B** Representation of the QD-ConA conjugates binding to structural components of the fungal cell wall. Representative images of *C. albicans* biofilms (**C**) and yeast cells (**D**) labeled with the QD-ConA conjugates, acquired using confocal fluorescence microscopy. Scale bars: 30 and 10 µm. The asterisk represents the extracellular matrix, and the arrow points to a hypha. **C** and **D** were reproduced with permission from Elsevier (Tenório et al. 2015)

red-emitting QDs (660 nm, d ~ 3.6 nm), through two conjugation methodologies: adsorption interaction or covalent binding. To conjugate the QDs with the lectin using adsorption interaction, the pH of the QD suspension was adjusted to 7.0 or 8.0, and Cramoll was added to the samples at a final concentration of 280 µg/mL. To perform the conjugation by covalent binding, the QD suspension (at pH 5.5) was mixed with EDC and sulfo-NHS, and after 15 min, Cramoll was added at the same concentration as before. Subsequently, the pH of the nanosystems, prepared by covalent coupling, was adjusted to a range of 6.0 to 7.4 to identify the pH at which the conjugate would exhibit chemical stability and promote the highest cell labeling.

As in the previous study using ConA, *C. albicans* cell suspensions (1×10^6 CFU/mL) were incubated with the QD-Cramoll nanosystem at 1:1 (v/v, cell:conjugate) for 1 h. Before incubation with cells, the carboxylic moieties of QDs, that did not react with the lectin, were blocked with TRIS-base (1 mmol/L) for 1.5 h to minimize non-specific binding in conjugates prepared using covalent binding. Flow cytometry and fluorescence microscopy were used to select the optimal conjugate.

The authors reported that none of the conjugates prepared by covalent coupling were effective, with the best one labeling no more than 17% of the cells. In contrast, the most effective labeling, covering about 92% of the cells, was achieved with the conjugate prepared by adsorption interaction at pH 7.0, which also led to intense cell staining under fluorescence microscopy. Moreover, no change in HA results was observed compared to the lectin alone, indicating that the Cramoll biological function was preserved after the conjugation. To confirm specificity, an inhibition assay was performed by pre-incubating the conjugate with methyl-α-D-mannopyranoside (0.4 mol/L) for 30 min before cell interaction. Under these conditions, a reduction in labeling from 92% to around 3% was observed, due to the inhibition of the lectin's CRD, demonstrating the specificity of the conjugate.

Cramoll and ConA share structural and carbohydrate recognition similarities. However, their pIs differ: Cramoll has a pI of 8.5–8.6, while ConA has a pI of approximately 5.7. As a result, under physiological pH, Cramoll is positively charged, making electrostatic interactions likely the driving force for its adsorption onto the negatively charged carboxyl-coated QDs used in this study. In contrast, ConA, being negatively charged under similar conditions, is less likely to interact electrostatically. Instead, other interactions, such as hydrogen bonds, may play a more prominent role in ConA adsorption to QDs (Cunha et al. 2018).

On the other hand, Oliveira et al. (2020a) conjugated QD green-emitting (571 nm, d ~ 2.8 nm, at pH 7.0) with Cramoll (at a final concentration of 280 µg/mL) and applied the nanosystem to assess the glucose/mannose profile of *C. albicans*, *C. glabrata* (recently named *Nakaseomyces glabrata*), and *C. parapsilosis*. The QD-Cramoll conjugates, incubated with 1×10^6 CFU/mL of fungal suspension (1:1, v/v) for 1 h, labeled approximately 92% of *C. albicans* and *C. glabrata* cells. Labeling inhibition was observed when conjugates were incubated with methyl-α-D-mannopyranoside (0.4 mol/L) for 30 min before being added to the cell suspensions. Interestingly, about 97% of *C. parapsilosis* cells were labeled by the nanosystem, but even after inhibition with methyl-α-D-mannopyranoside, 78% of the labeling persisted. The authors noted that the Cramoll lower affinity for monovalent carbohydrates, like methyl-α-D-mannopyranoside, does not promote sufficient inhibition, as *C. parapsilosis* cells may have higher amounts of exposed carbohydrates organized in multivalent domains (cluster effect). Therefore, QD-Cramoll conjugates proved to be an effective fluorescent nanoprobe for evaluating the glucose/mannose profile of fungal cell walls, particularly in species frequently associated with candidiasis (Oliveira et al. 2020a).

Cryptococcus neoformans primarily causes cryptococcosis, with manifestations ranging from pulmonary infections to life-threatening meningoencephalitis, particularly in immunocompromised individuals, such as those with HIV/AIDS or undergoing immunosuppressive therapy (WHO 2022). *C. neoformans* was also used as a biological model in the development of conjugates involving red-emitting QDs (*ca.* 653 nm and d ~ 3.7 nm) and SteLL or PgTeL lectins that have an affinity to chitin and glycoproteins, respectively (Silva et al. 2021a). This choice was based on the presence of chitin residues in the cell wall of this fungus (Garcia-Rubio et al. 2020). SteLL and PgTeL exhibit distinct global charges, with pIs of approximately 5.7 and 6.5, respectively. Consequently, the authors investigated optimal conjugation through adsorption interactions at various pH levels, incubating lectins (starting concentrations of 2.0 mg/mL and 3.1 mg/mL for SteLL and PgTeL, respectively) in a ratio of 1:5 (lectins:QDs, v/v). Notably, QD-SteLL (at pH 7.0) and QD-PgTeL (at pH 8.0) nanosystems demonstrated high colloidal stability and fluorescence, along with the absence of precipitation. These conditions were utilized in further assays.

An FMA was conducted, yielding *RF* values of 1262% for the QD-PgTeL and 374% for the QD-SteLL conjugates, compared to free lectins and non-conjugated QDs, which indicated that successful conjugations were achieved. Furthermore, QD-SteLL and QD-PgTeL conjugates also remained functional after exposure to denaturing agents, including temperature and urea, showing results like those of the free lectins.

To evaluate the specificity of the nanosystems, they were inhibited by a 30-min incubation with glycoproteins (fetuin, azocasein, or ovalbumin at 0.4 mg/mL) before contact with the cells. Binding remained unaffected in the presence of GlcNAc (100 mmol/L), the monomeric base of chitin

polymers. The labeling was analyzed using flow cytometry. Approximately 1×10^5 CFU/mL of *C. neoformans* cells were incubated with the conjugates in a 1:1 volume ratio for 1 h, resulting in about 99% of cells being labeled by the QD-SteLL nanosystem. Following incubation with GlcNAc, the labeling persisted in 93% of the cells.

Additionally, the presence of fetuin, ovalbumin, or azocasein inhibited the labeling to levels of about 20, 14, and 17%, respectively, demonstrating the specificity of the nanosystem. Similar results were observed for the QD-PgTeL conjugates, which labeled 99% of *C. neoformans* cells. The labeling percentages were approximately 94, 12, 23, and 9% after inhibition, respectively, by GlcNAc, fetuin, ovalbumin, and azocasein. At last, fluorescence microscopy revealed that the surface of *C. neoformans* cells was intensely stained by the nanotools. This study highlighted the potential of the prepared conjugates for future research on microbial infections and pathogen monitoring (Silva et al. 2021a).

Candida albicans was also applied as a biological model in the development of a conjugate based on QDs (emission peak at 667 nm and d ~ 4.2 nm) and a recombinant human mannose-binding lectin (rhMBL) (Lima et al. 2022). As reported in the "Lectins" section, MBL lectin binds to specific regions of mannose, L-fucose, GlcNAc, and ManNAc. The authors evaluated different conjugation strategies: adsorption interaction at different pH values of the QD suspension (4.5, 6.0, and 7.0) and covalent binding using the coupling agents EDC and NHS. The rhMBL (1 mg/mL) was added to the QD suspension to achieve a final lectin concentration of 50 µg/mL. The conjugation efficiency was assessed by incubating *C. albicans* yeast cells (about 1×10^6 CFU/mL) with the nanosystems at a 1:1 (v/v) ratio for 30 min, ensuring that carboxyl groups from the conjugates prepared using covalent binding were blocked with TRIS-base prior to incubation with the fungal cells. Thus, flow cytometry results revealed that the conjugate obtained by adsorption interaction at pH 6.0 was the most efficient since it promoted the highest labeling percentage and median of fluorescence intensity of *C. albicans*, respectively, *ca.* 100% and 8×10^5 arbitrary units.

MBL is a C-type lectin, that is, it requires calcium to perform its action (Idowu et al. 2021). Thus, the conjugate was incubated with fungal cells under different conditions: (i) medium containing saline solution 0.9% (w/v) without calcium, (ii) with calcium, or (iii) with calcium plus ethylenediaminetetraacetic acid (EDTA) to chelate these ions. Furthermore, the specificity of the QD-rhMBL nanoprobe was investigated by pre-incubating the conjugate with 0.4 mol/L of methyl-α-D-mannopyranoside or mannan in the presence of calcium ions for 30 min to inhibit CRDs of the lectin, before binding to yeast cells. In these assays, cell suspensions were incubated for 15 min with the conjugate at a ratio of 5:1 (v/v, cell:conjugate). The authors found that effective labeling of *C. albicans* with the conjugate required the presence of calcium ions in the incubation solution, since without it or when it was chelated by EDTA, labeling did not occur. Moreover, the inhibition of rhMBL in the conjugate by the monosaccharide methyl-α-D-mannopyranoside was not effective, while pre-incubation with the polysaccharide mannan sharply reduced the labeling. These results suggested that the arrangement of carbohydrate residues forming clusters, such as those present on the surface of pathogens, is preferentially recognized by rhMBL (cluster effect). In addition, conventional fluorescence microscopy revealed homogeneous labeling of the cell surface by the best conjugate. Given the role of MBL in the innate immune system by collaborating with the elimination of pathogenic microorganisms and apoptotic cells, this conjugate may serve as a valuable tool for fluorescent monitoring of MBL action. It could support studies aimed at elucidating MBL-related mechanisms in disease and infection (Lima et al. 2022).

Bacteria

Aeromonas is a bacterial genus of Gram-negative bacteria that naturally inhabit aquatic environments, acts as fish pathogens, and can pose a threat to aquaculture (Pessoa et al. 2019). In addition, these bacteria can cause opportunistic infections in humans and have been gaining prominence in the medical literature (Pessoa et al. 2022). Since glycostructures on the bacterial surface may be involved in virulence as well as host–pathogen interaction, Pessoa et al. (2023) used the QD-Cramoll nanosystem to study the glucose/mannose profile in four *Aeromonas* spp. (*A. hydrophila*, *A. caviae*, *A. dhakensis*, and *A. jandaei*) isolated from *Colossoma macropomum* (Tambaqui fish) (Pessoa et al. 2023).

The QDs used in the conjugate preparation had an estimated size of *ca.* 3.4 nm and exhibited a maximum emission peak at 621 nm. The bacterial suspensions prepared in saline solution (5×10^6 CFU/mL) were incubated with the conjugate in a ratio of 1:1 (v/v) for 1 h. The specificity of the labeling was evaluated by inhibition assay pre-incubating the conjugate with methyl-α-D-mannopyranoside (0.4 mol/L) or mannan (0.2 mol/L) for 1 h before contact with the bacterial cells. Through flow cytometry analyses to quantify the fluorescent labeling of *Aeromonas* strains by the conjugate, the authors inferred that *A. jandaei* and *A. dhakensis* possess higher glucose/mannose content and/or more accessible carbohydrate sites, as the QD-Cramoll conjugates labeled approximately 90 and 77% of the cells, respectively. In contrast, *A. caviae* (*ca.* 62%) and *A. hydrophila* (*ca.* 56%) showed lower levels of staining. The authors suggested that this labeling difference may be mediated by variations in glycoconjugates on the *Aeromonas* cell surface, such as lipopolysaccharide (LPS), as shown in Fig. 3. The carbohydrate composition of LPSs remains incompletely characterized

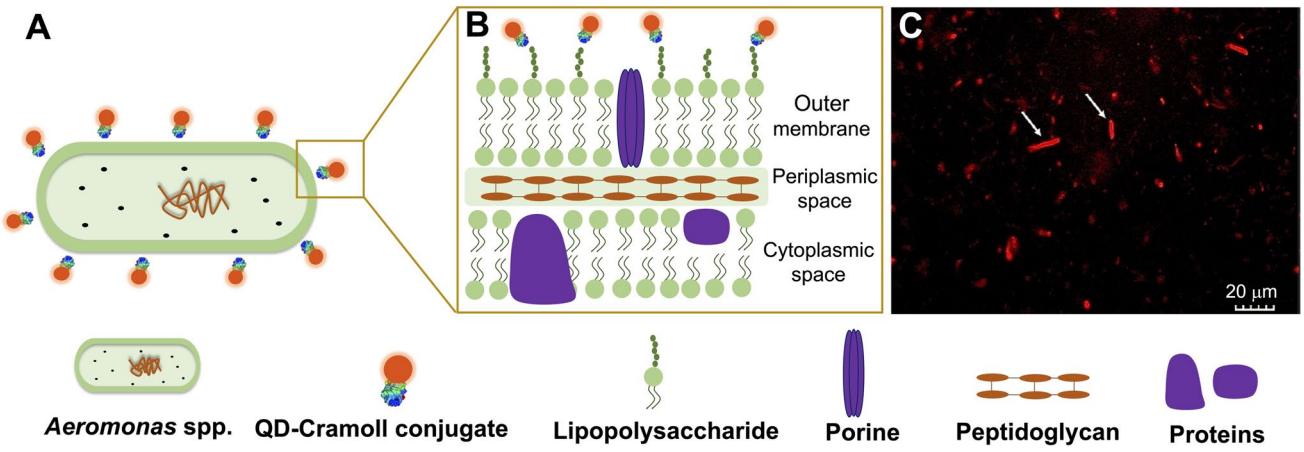

Fig. 3 **A** Schematic overview of the *Aeromonas* cell surface and the interaction of QD-Cramoll conjugates with glucose/mannose residues in glycostructures such as lipopolysaccharide. **B** A zoomed-in view of the cell surface. **C** Representative image of *A. jandaei* labeled with the QD-Cramoll conjugates acquired using a confocal fluorescence microscopy, scale bar: 20 µm. **C** was reproduced with permission from Elsevier (Pessoa et al. 2023)

across different species. Thus, the authors demonstrated the efficiency of a lectin-based conjugate to sensitively investigate and differentiate the glycophenotype of *Aeromonas* bacterial species (Pessoa et al. 2023).

In another approach to the application of lectin-based conjugates, Silva et al. (2024) tested the antimicrobial and antibiofilm activities of the PgTeL against *Pseudomonas aeruginosa*, a bacterium that causes nosocomial infections in humans. Additionally, the QD-PgTeL conjugates were used to investigate the lectin interaction with glycoconjugates present in planktonic cells as well as biofilms. The lectin had a bacteriostatic and bactericidal effect on *P. aeruginosa* in both the non-resistant (ATCC 27853) and multidrug-resistant strains (UFPEDA 261 and UFPEDA 262), presenting minimal inhibitory concentrations (MICs) of 12.5 (sensible) and 25 µg/mL (resistant). Furthermore, this lectin displayed activity in inhibiting biofilm formation (greater than 50%) and against preformed biofilms of the three strains, according to analyses using crystal violet.

To investigate the interaction of the PgTeL with the cell surface of *P. aeruginosa*, this lectin was conjugated with QDs of d ~ 3.2 nm and a maximum emission peak at 610 nm. Bacterial suspensions (about 3×10^6 CFU/mL) were incubated with the QD-PgTeL conjugates in a 1:1 (v/v) ratio for 1 h. The investigation of the involvement of the lectin's CRD in the interaction with bacteria was evaluated by an inhibition assay, performed before incubating the conjugate with bacteria. For this, the conjugate was previously incubated for 30 min with fetuin (0.4 mg/mL), a glycoprotein for which PgTeL has an affinity. Furthermore, after treating the biofilms with PgTeL at their respective MICs, the biofilms were washed and incubated with the QD-PgTeL nanosystem for 30 min. The inhibition of the conjugate with fetuin was also performed as previously mentioned. Using flow cytometry, greater labeling was observed in the multidrug-resistant strains (*ca.* 74% for UFPEDA 261 and *ca.* 55% for UFPEDA 262) compared to the non-resistant one (about 45%). Furthermore, when the conjugate was previously inhibited by fetuin, there were significant decreases in the labeling percentages, suggesting that the binding to bacterial cells by PgTeL occurs through the CRD of the lectin. It is known that *P. aeruginosa* has glycoproteins and glycolipids in its membrane, and this bacterium also has the virulence factor LPS consisting of an inner core, named lipid A, an outer core, and the O antigen or polysaccharide (González-Alsina et al. 2023). Thus, Silva and collaborators proposed that the differences in labeling (UFPEDA 261 > UFPEDA 262 > ATCC 27853) among the strains tested may be due to differences in the compositions of cell surface glycoconjugates. In confocal fluorescence microscopy of *P. aeruginosa* biofilms, those not treated with the lectin exhibited bright labeling and an unchanged structure after incubation with QD-PgTeL conjugates, while biofilms previously treated with the lectin exhibited a decreased fluorescence, suggesting structural impairment and/or biofilm disturbance induced by PgTeL. Therefore, the conjugate proved to be an efficient tool to elucidate the involvement of the PgTeL's CRD with the cell surface of different *P. aeruginosa* strains, estimate the composition of glycoconjugates as well as analyze the biofilm structure (Silva et al. 2024).

Red blood cells

RBCs are responsible for transporting O_2 and CO_2 in the bloodstream and possess a rich molecular surface, which also includes carbohydrates (Lee-Sundlov et al. 2020). Sialic

acid (SA), for example, is a structural carbohydrate responsible for the negative Zeta potential of RBCs, which prevents them from interacting with endothelial cells and other RBCs, thus avoiding blood clots (Ghosh 2020; Doostkam et al. 2022).

In addition to SA, RBCs also possess other carbohydrates, such as those associated with antigens of the ABO system (Lee-Sundlov et al. 2020). These carbohydrates can be used to characterize RBCs into different groups, such as A_1, B, A_1B, or O. The precursor of the A_1 and B antigens is the H antigen, which has in its composition exposed L-fucose residues. To produce the A_1 antigen, the enzyme α(1,3)*N*-acetylgalactosaminyltransferase inserts an *N*-acetylgalactosamine to the H antigen. On the other hand, when the enzyme α(1,3)galactosyltransferase transfers galactose to the H antigen, the B antigen is formed. O group does not possess an active enzyme, and thus the H determinant remains unchanged on RBCs. Therefore, a better understanding of the H antigen profile in RBCs can enhance our understanding of their biology as well as aspects related to blood groups (Yazer et al. 2006).

In a study conducted by Cabral Filho et al. (2015), green-emitting QDs were covalently conjugated to *Ulex europaeus* agglutinin I (UEA-I), a lectin with an affinity for L-fucose, and the nanosystem was applied to quantify and understand the pattern of H antigen in RBCs. For the conjugation, EDC and sulfo-NHS were added to the QD suspension (at pH 5.5) to activate their carboxylic groups. Then, UEA-I was added to the mixture, resulting in the QD-UEA-I conjugates. The final concentration of this lectin in the nanosystem was 30 µg/mL.

The QDs exhibited an emission peak at 548 nm and presented d ~ 2.6 nm. The conjugation between QDs and UEA-I was also evaluated by FCS, where the hydrodynamic diameters of QDs and the conjugate were determined based on the diffusion times of these nanostructures. The hydrodynamic diameter from the conjugated QDs was about 10 × larger than that of non-conjugated QDs, indicating that the lectin interacted with the QD surface.

The conjugate was incubated with TRIS-base for 2 h to block any activated carboxyl groups on the QD surface that did not react with UEA-I. Then, the conjugate was added to 1% (v/v) suspensions of RBCs of different ABO blood groups (O, A_1, A_1B, B, and A_{weak} groups, like A_2, A_x, and A_{el} phenotypes). Investigating antigens in A_{weak} subgroups is important, for example, to improve transfusion safety procedures. All these different groups were incubated with QD-UEA-I conjugates for 1 h, at 37 °C. The ratio used was 1:1 (v/v, conjugate:cells). A_1 and B groups were used as controls because they have a very low H antigen exposed on their surfaces. Moreover, an inhibition assay was performed to assess the specificity of the nanosystem by interacting QD-UEA-I conjugates with L-fucose (0.3 mol/L) for 1 h. The inhibited system was then incubated with O RBCs. The interaction of the conjugate with RBCs was evaluated by flow cytometry.

Approximately 85% of O RBCs were labeled by the conjugate. A_1, B, and A_1B RBCs, on the other hand, showed less expressive labeling, as expected, below 8%. The lower labeling of these groups can be explained by the fact that almost all H antigens, which contain L-fucose moieties, have been converted into A or B antigens. A_{weak} types, such as A_x and A_{el}, were also evaluated and exhibited 30% of labeling. On the other hand, the A_2 type showed 70% labeling. The interaction of A_2 RBCs with QD-UEA-I conjugates occurred because the lectin can recognize L-fucose that has not yet been converted to A_2 antigen. In addition, the L-fucose in this antigen is more exposed.

Furthermore, it is worth noting that when UEA-I from the conjugates was inhibited with L-fucose, the nanosystem was unable to interact with O RBCs, indicating specificity. Thus, the QD-UEA-I nanosystem is a tool capable of identifying and quantifying H antigens in RBCs, even in A_{weak} subgroups, allowing for more precise characterization of these cells. In this study, orange QDs (emission peak at 610 nm and d ~ 3.1 nm) were also conjugated with anti-A or anti-B antibodies. The QD-anti-A and QD-anti-B nanosystems were used to study the A_1 and B antigens distribution in different ABO blood groups. The conjugates developed can be used as complementary and versatile tools for comprehending erythrocyte biology and contributing to advances in the immunophenotyping of blood systems (Cabral Filho et al. 2015).

In another study with RBCs, Oliveira et al. (2020b) conjugated QDs with BmoLL, a galactose-binding lectin. The lectin was added to QD suspensions at pH 7.0 and 8.0 to evaluate the best conditions to conjugate the compounds by adsorption interaction. When BmoLL was added at pH 7.0, the colloidal stability of the nanosystem was compromised. Therefore, only the nanosystem prepared at pH 8.0 was studied. The QD-BmoLL nanosystem is illustrated in Fig. 4A. The final concentration of BmoLL in this system was 280 µg/mL. QDs displayed a maximum emission at 617 nm and d ~ 3.3 nm. The biological activity of the lectin conjugated to the QDs was assessed by the HA assay. After conjugation, BmoLL retained its biological activity, showing a hemagglutination capacity like that of the free lectin.

To evaluate the ability of the QD-BmoLL conjugate to interact with galactose, A_1, A_1B, B, and O RBCs were used as biological models. The authors hypothesized that B and A_1B RBCs could interact with the QD-BmoLL conjugates because they have B antigen, which contains exposed galactose residues on its structure. On the other hand, A_1 and O RBCs would not interact with the nanosystem, as there is no significant amount of exposed galactose residues on the surface of these cells. To confirm

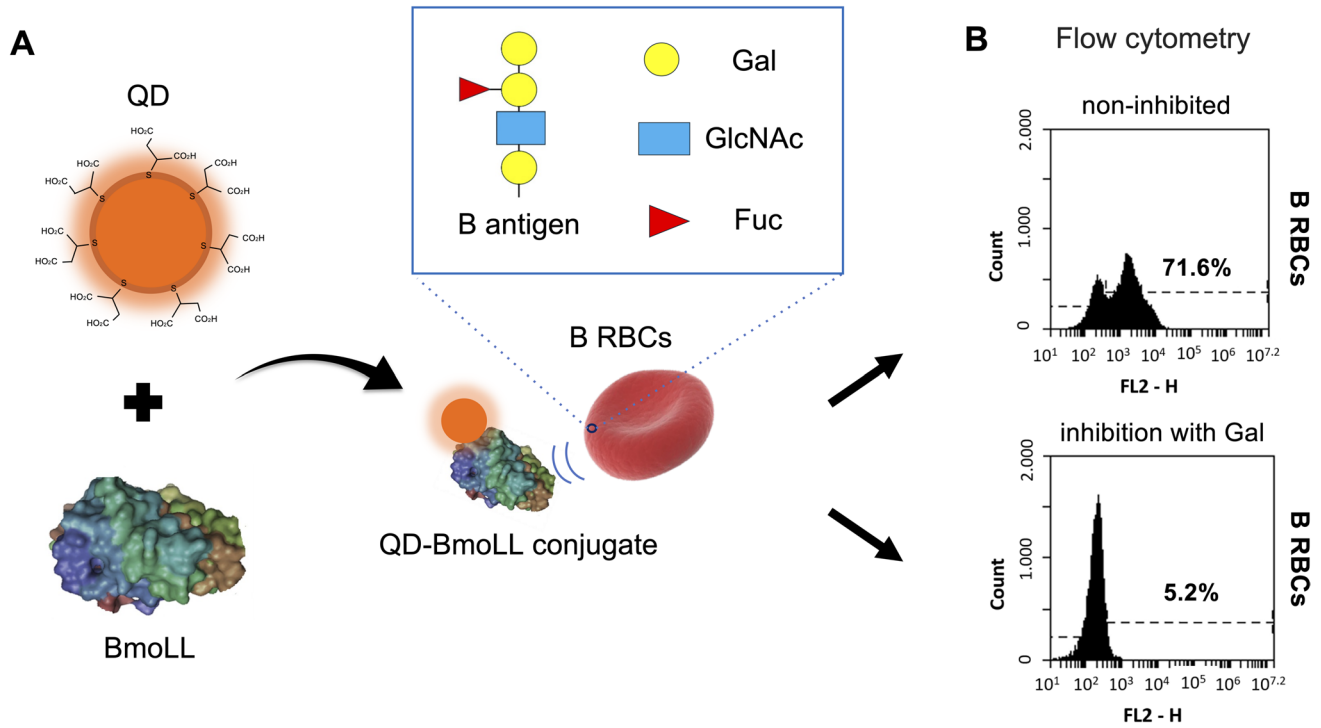

Fig. 4 **A** Representation of the QD-BmoLL conjugate and its interaction with B RBCs. The constituents of B antigen are also illustrated. **B** The labeling by flow cytometry of B RBCs by inhibited and non-inhibited QD-BmoLL conjugates is shown. Gal, galactose; Fuc, L-fucose; GlcNAc, *N*-acetyl-D-glucosamine. **B** was reproduced with permission from IOP Publishing (Oliveira et al. 2020b)

the specificity of the interaction between the conjugate and RBCs, an inhibition assay was performed, in which the BmoLL binding sites were inhibited with galactose (0.2 mol/L) for 30 min. The labeling of RBCs by QD-BmoLL conjugates was measured by flow cytometry. Both systems (inhibited and non-inhibited QD-BmoLL conjugates) were incubated with the RBCs at a 1:1 v/v ratio for 1 h. The nanosystem was unable to significantly bind to A_1 and O RBCs, exhibiting labeling lower than ~ 3%. In type B cells, the labeling was approximately 70% (Fig. 4B). B RBCs after incubation with the nanosystem, in which BmoLL was inhibited by galactose, showed labeling of *ca.* 6% (Fig. 4B). Although A_1B cells display A_1 and B antigens simultaneously (i.e., they present galactose), QD-BmoLL conjugates labeled about 14% of A_1B RBCs. This result can be explained by the presence of *N*-acetylgalactosamine (A antigen) on A_1B cells, which can cause steric hindrance, making the interaction between galactose and BmoLL more difficult. These results suggest that the QD-BmoLL nanosystem was specific for galactose. Thus, the QD-BmoLL conjugate is a promising fluorescent probe for investigating the involvement of galactose not only in hematological conditions but also in glycobiological studies, including those associated with tumorigenesis and microbial pathogenicity mechanisms (Oliveira et al. 2020b).

Breast tissues

The glycans on cell membranes and the extracellular matrix play important roles in biological processes, and alterations associated with these molecules have been linked to the development of various diseases (Pinho et al. 2023). In cancer, for example, changes in the cellular metabolism have been related to carbohydrate profiles, influencing the tumor progression and prognosis of this disease (Kremsreiter et al. 2021). Hence, the ability of lectins to bind to carbohydrates, combined with the fluorescent properties of the QDs, can be useful for evaluating the glycocode of both healthy and diseased tissues.

Andrade et al. (2013) used QDs conjugated to ConA or UEA-I to investigate the glycan profile of human breast tissues (normal, fibroadenoma (benign), and invasive ductal carcinoma, IDC). These lectins were chosen because ConA has an affinity for glucose/mannose residues, while UEA-I binds to L-fucose moieties. QDs were conjugated to ConA (final concentration of 280 µg/mL) through adsorption interaction (at pH 8.0) and with UEA-I (final concentration of 140 µg/mL) by covalent binding (at pH 5.5) using EDC and

sulfo-NHS as coupling agents. QDs showed a maximum emission at 644 nm and d ~ 3.5 nm. An HA assay was performed to confirm that the ability of the lectins to bind to carbohydrates was not lost during conjugation. The conjugates and lectins displayed similar performance, suggesting that the carbohydrate recognition capabilities of ConA and UEA-I sites were preserved after conjugation.

Normal, fibroadenoma and IDC tissue slices were deparaffinized with xylene, hydrated in graded alcohols, treated with trypsin, and incubated with QD-ConA or QD-UEA-I conjugates (100 µL) for 2 h at 4 °C, followed by washing with PBS. An inhibition assay was also performed by incubating the QD-ConA and QD-UEA-I nanosystems, respectively, with methyl-α-D-mannopyranoside and L-fucose (0.3 mol/L for 1 h), prior to adding them to the tissues. A significant decrease in the fluorescence signal was observed in the samples, indicating that the conjugates interacted in a specific way with the tissues.

In contrast, fluorescence microscopy analyses indicated that QD-ConA conjugates bound preferentially to the stroma in all analyzed tissues. On the other hand, QD-UEA-I conjugates bound to ductal cells, especially in IDC samples. Thus, the conjugates were able to bind and map carbohydrates in human breast tissues, stimulating the evaluation of other QD-lectin conjugates for this purpose (Andrade et al. 2013).

In another study, Carvalho et al. (2019) used QDs conjugated with Cramoll to evaluate the glucose/mannose profile of human breast tissues (normal, fibroadenoma, and IDC). For this, QDs were conjugated to Cramoll as previously described (Oliveira et al. 2020a; Pessoa et al. 2023). The QDs displayed a maximum emission wavelength at 655 nm and d ~ 3.6 nm. The labeling of *C. albicans* yeast cells confirmed that a successful conjugation was reached. Moreover, a circular dichroism analysis indicated that the lectin's secondary structure remained preserved even after conjugation with the QDs. An HA assay also confirmed that Cramoll retained its biological activity after interacting with the QDs.

QD-Cramoll conjugates (Fig. 5A) were then applied to investigate the glycocode of the breast tissues. The slices were deparaffinized using xylene, hydrated in graded alcohols, treated with trypsin, and incubated with QD-Cramoll nanosystems (100 µL) for 30 min at 4 °C. The specificity of the conjugate was also evaluated using the tissues in inhibition and saturation assays. For the inhibition assay,

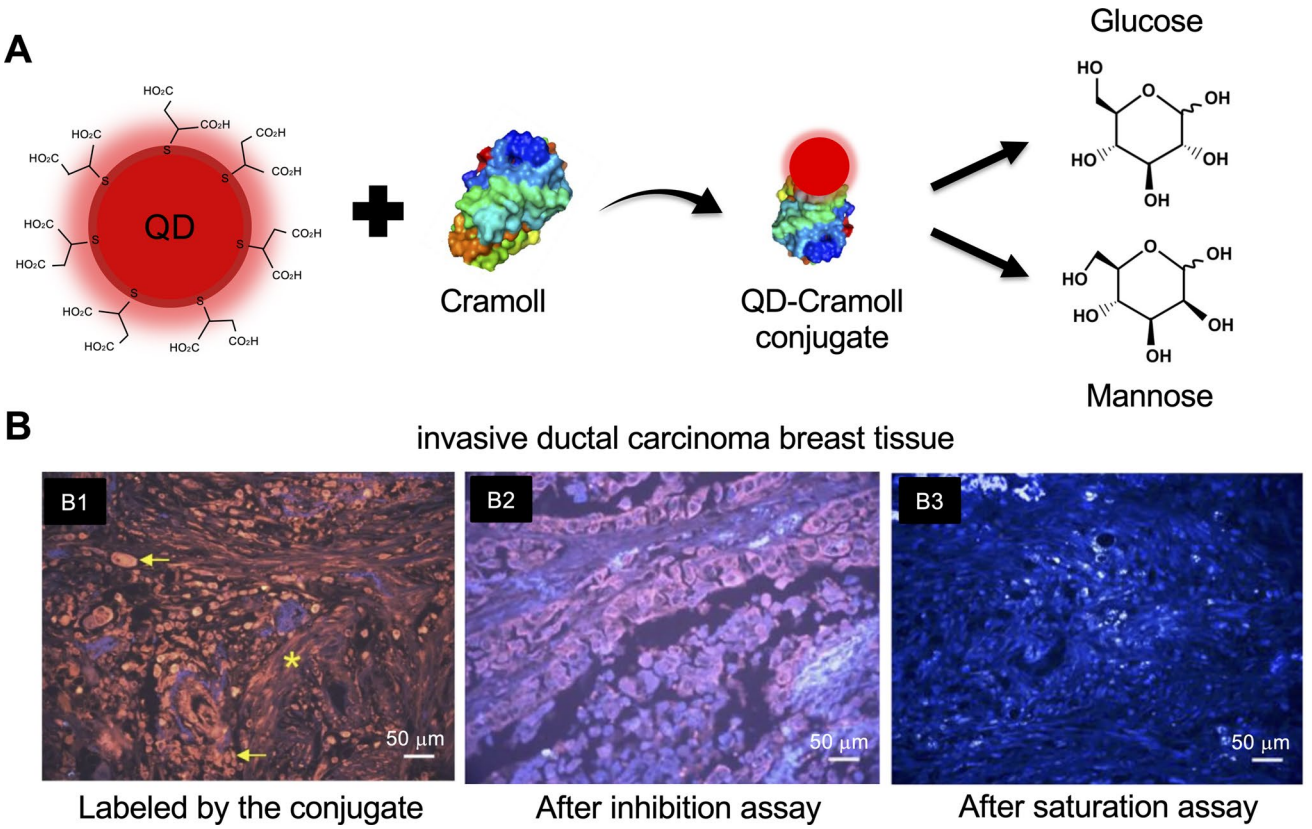

Fig. 5 **A** Schematic illustration of the QD-Cramoll conjugate. **B** Representative fluorescence microscopy images of invasive ductal carcinoma human breast tissues labeled with QD-Cramoll conjugates (B1), following the inhibition assay (B2), and after the saturation assay (B3). Asterisks represent stroma and the arrows point to cells. Scale bars: 50 µm. Figures 5B1, 5B2, and 5B3 were reproduced with permission from Elsevier (Carvalho et al. 2019)

the nanosystem was previously incubated with methyl-α-D-mannopyranoside (0.4 mol/L). For the saturation assay, the slices were incubated with an excess of Cramoll (140 mg/mL, for 2 h, at 4 °C), and then the conjugate was added. Fluorescence microscopy analyses showed an intense labeling of IDC breast tissues, in both ductal cells and stroma, indicating a high presence of glucose/mannose residues in these tissues. It was also observed that the conjugate labeled preferentially ductal cells in normal and fibroadenoma breast tissues. The microscopy analyses demonstrated that QDs-Cramoll conjugates were able to reveal different labeling and glucose/mannose patterns in IDC and fibroadenoma samples. A quantitative measurement was also proposed in the study by using a fluorescence microplate reader to quantify the signal in the tissues. For this, the slices were processed as before and then transferred to 96-well black polystyrene microplates that had been pre-filled with PBS. A higher fluorescence signal was noticed in IDC samples, corroborating the fluorescence microscopy analyses.

In the inhibition assay, a residual fluorescence was observed in tissues (mainly IDC), which could be explained by the higher affinity of lectins for complex carbohydrates (cluster effect), compared to monosaccharides, such as methyl-α-D-mannopyranoside. No fluorescence from the conjugate was visualized after the saturation assay. Representative images for IDC tissue are shown in Fig. 5B. The results indicated that the conjugate-tissue interaction was specific, enabling the investigation of glucose/mannose profiles in different types of human breast tissues, as can be observed in Carvalho et al. (2019).

Conclusion

Carboxylated CdTe/CdS QDs have been conjugated with native (purified from plants) or recombinant lectins with different specificities, mainly by the adsorption approach. It is important to use a biological model that contains carbohydrates known to be recognized by the lectin conjugated to the QDs to evaluate the labeling efficiency of the QD-lectin conjugates. Furthermore, inhibition assays are also relevant to confirm that the formulated conjugate promotes specific glycobiological labeling.

QD-lectin conjugates have proven to be versatile optical tools for a wide range of glycobiological studies, such as glycophenotype characterization of yeast and bacterial cell walls, cancerous tissues, and erythrocyte antigens. Moreover, the brightness of lectins upon conjugation with QDs can provide insights into their biological action. Therefore, QD-lectin conjugates are emerging as promising nanoprobes for carbohydrate studies, allied with fluorescence-based techniques that provide highly sensitive tools for molecular investigations.

Acknowledgements JVAL thanks the Fundação Coordenação de Aperfeiçoamento de Pessoal de Nível Superior for his scholarship (CAPES, Finance Code 001). WFO and FPTM thank the Conselho Nacional de Desenvolvimento Científico e Tecnológico (CNPq) for their scholarships. AF, PECF, and MSR also thank CNPq for their Productivity in Research fellowships. ARS thanks Fundação de Amparo à Pesquisa do Estado de São Paulo for his scholarship (FAPESP, grant # 2021/14119-6).

Author contributions All authors contributed equally to this manuscript. All authors were responsible for conceptualization, methodology, writing, and revising the review.

Funding Comissão Nacional de Energia Nuclear,Instituto Nacional de Fotônica,465763/2014-6,465763/2014-6,465763/2014-6,Conselho Nacional de Desenvolvimento Científico e Tecnológico,Fundação de Amparo à Ciência e Tecnologia do Estado de Pernambuco

Data availability No datasets were generated or analysed during the current study.

Declarations

Competing interests The authors declare no competing interests.

References

Adegoke O, Nyokong T, Forbes PB (2015) Structural and optical properties of alloyed quaternary CdSeTeS core and CdSeTeS/ZnS core–shell quantum dots. J Alloy Compd 645:443–449. https://doi.org/10.1016/j.jallcom.2015.05.083

Agarwal K, Rai H, Mondal S (2023) Quantum dots: an overview of synthesis, properties, and applications. Mater Res Exp 10:062001. https://doi.org/10.1088/2053-1591/acda17

Ahmmed MK et al (2022) An update of lectins from marine organisms: characterization, extraction methodology, and potential biofunctional applications. Mar Drugs 20:430. https://doi.org/10.3390/md20070430

Aladesuyi O et al (2022) Biological applications of ternary quantum dots: a review. Nanotechnol Rev 11:2304–2319. https://doi.org/10.1515/ntrev-2022-0136

Andrade CG et al (2013) Evaluation of glycophenotype in breast cancer by quantum dot-lectin histochemistry. Int J Nanomed 2013:4623–4629. https://doi.org/10.2147/IJN.S51065

Bilan R et al (2017) Quantum-dot-based suspension microarray for multiplex detection of lung cancer markers: preclinical validation and comparison with the Luminex xMAP® system. Sci Rep 7:44668. https://doi.org/10.1038/srep44668

Bindeman WE, Fingleton B (2022) Glycosylation as a regulator of site-specific metastasis. Cancer Metastasis Rev 41:107–129. https://doi.org/10.1007/s10555-021-10015-1

Cabral Filho PE et al (2015) Blood group antigen studies using CdTe quantum dots and flow cytometry. Int J Nanomed 4393–4404. https://doi.org/10.2147/IJN.S84551

Cabral Filho PE et al (2018) Multimodal highly fluorescent-magnetic nanoplatform to target transferrin receptors in cancer cells. Biochim Biophys Acta (BBA) Gen Subj 1862:2788–2796. https://doi.org/10.1016/j.bbagen.2018.08.014

Carvalho KHG et al (2014) Fluorescence plate reader for quantum dot-protein bioconjugation analysis. J Nanosci Nanotechnol 14:3320–3327. https://doi.org/10.1166/jnn.2014.8721

Carvalho MET et al (2019) Evaluating the glycophenotype on breast cancer tissues with quantum dots-Cramoll lectin conjugates. Int J

Biol Macromol 138:302–308. https://doi.org/10.1016/j.ijbiomac.2019.07.088
Cavada BS et al (2019) One century of ConA and 40 years of ConBr research: a structural review. Int J Biol Macromol 134:901–911. https://doi.org/10.1016/j.ijbiomac.2019.05.100
Chettri D et al (2021) Lectins: biological significance to biotechnological application. Carbohyd Res 506:108367. https://doi.org/10.1016/j.carres.2021.108367
Coelho LCBB, Silva MB (2000) Simple method to purify milligram quantities of the galactose-specific lectin from the leaves of Bauhinia monandra. Phytochem Anal 11:295–300. https://doi.org/10.1002/1099-1565(200009/10)11:5%3c295::AID-PCA517%3e3.0.CO;2-S
Correia MTS and Coelho LCBB (1995) Purification of a glucose/mannose specific lectin, isoform 1, from seeds of Cratylia mollis Mart. (Camaratu Bean). Appl Biochem Biotechnol 55:261–273. https://doi.org/10.1007/BF02786865
Cunha CRA et al (2018) Quantum dot–Cramoll lectin as novel conjugates to glycobiology. J Photochem Photobiol B 178:85–91. https://doi.org/10.1016/j.jphotobiol.2017.10.020
Cunningham BA et al (1975) The covalent and three dimensional structure of concanavalin A. II. Amino acid sequence of cyanogen bromide fragment F3. J Biol Chem 250:1503–1512. https://doi.org/10.1016/S0021-9258(19)41841-3
Da Costa PFGM et al (2024) Real-time monitoring of CdTe quantum dots growth in aqueous solution. Sci Rep 14:7884. https://doi.org/10.1038/s41598-024-57810-8
De Coninck T, Van Damme EJM (2021) Review: the multiple roles of plant lectins. Plant Sci 313:111096. https://doi.org/10.1016/j.plantsci.2021.111096
De Thomaz AA, Almeida DB, Cesar CL (2014) Measuring the hydrodynamic radius of quantum dots by fluorescence correlation spectroscopy. In: Fontes A, Santos B (eds) Quantum dots: applications in biology, 2rd edn. Humana Press, New York, pp 85–91. https://doi.org/10.1007/978-1-4939-1280-3_6
Doostkam A et al (2022) Sialic acid: an attractive biomarker with promising biomedical applications. Asian Biomed 16:153–167. https://doi.org/10.2478/abm-2022-0020
Fernandes PAR, Coimbra MA (2023) The antioxidant activity of polysaccharides: a structure-function relationship overview. Carbohyd Polym 314:120965. https://doi.org/10.1016/j.carbpol.2023.120965
Foubert A et al (2016) Bioconjugation of quantum dots: review & impact on future application. TrAC Trends Anal Chem 83:31–48. https://doi.org/10.1016/j.trac.2016.07.008
Freire MS et al (2024) Advances on chalcogenide quantum dots-based sensors for environmental pollutants monitoring. Sci Total Environ 931:172848. https://doi.org/10.1016/j.scitotenv.2024.172848
Garcia-Rubio R et al (2020) The fungal cell wall: Candida, Cryptococcus, and Aspergillus Species. Front Microbiol 10:2993. https://doi.org/10.3389/fmicb.2019.02993
Ghosh S (2020) Sialic acid and biology of life: an introduction. In: Ghosh S (ed) Sialic acids and sialoglycoconjugates in the biology of life, health and disease. Academic Press, pp 1–61. https://doi.org/10.1016/B978-0-12-816126-5.00001-9
Gidwani B et al (2021) Quantum dots: prospectives, toxicity, advances and applications. J Drug Deliv Sci Technol 61:102308. https://doi.org/10.1016/j.jddst.2020.102308
Gomez DE et al (1995) Ulex europaeus I lectin induces activation of matrix-metalloproteinase-2 in endothelial cells. Biochem Biophys Res Commun 216:177–182. https://doi.org/10.1006/bbrc.1995.2607
González-Alsina A et al (2023) Pseudomonas aeruginosa and the complement system: a review of the evasion strategies. Microorganisms 11:664. https://doi.org/10.3390/microorganisms11030664
Han YD et al (2014) Quantum dot and π-conjugated molecule hybrids: nanoscale luminescence and application to photoresponsive molecular electronics. NPG Asia Mater 6:e103. https://doi.org/10.1038/am.2014.28
Hanau S et al (2020) Schematic overview of oligosaccharides, with survey on their major physiological effects and a focus on milk ones. Carbohydr Polym Technol Appl 1:100013. https://doi.org/10.1016/j.carpta.2020.100013
Herrera-Ochoa D et al (2022) A novel quantum dot-based pH probe for long-term fluorescence lifetime imaging microscopy experiments in living cells. ACS Appl Mater Interfaces 14:2578–2586. https://doi.org/10.1021/acsami.1c19926
Hooper J et al (2022) Polyvalent glycan quantum dots as a multifunctional tool for revealing thermodynamic, kinetic, and structural details of multivalent lectin-glycan interactions. ACS Appl Mater Interfaces 14:47385–47396. https://doi.org/10.1021/acsami.2c11111
Idowu PA et al (2021) (2021) Activity of mannose-binding lectin on bacterial-infected chickens—a review. Animals 11(3):787. https://doi.org/10.3390/ani11030787
Ji Back G et al (2024) Green synthesis and luminescence characteristics of ZnSe-ZnS core-shell quantum dots. J Cryst Growth 626:127475. https://doi.org/10.1016/j.jcrysgro.2023.127475
Kaltner H et al (2019) The sugar code: letters and vocabulary, writers, editors and readers and biosignificance of functional glycan–lectin pairing. Biochem J 476:2623–2655. https://doi.org/10.1042/BCJ20170853
Kremsreiter SM et al (2021) Glycan–lectin interactions in cancer and viral infections and how to disrupt them. Int J Mol Sci 22:10577. https://doi.org/10.3390/ijms221910577
Lee-Sundlov MM, Stowell SR, Hoffmeister KM (2020) Multifaceted role of glycosylation in transfusion medicine, platelets, and red blood cells. J Thromb Haemost 18:1535–1547. https://doi.org/10.1111/jth.14874
Li H et al (2023) Quantum dots for optoelectronics. Adv Photonics 5:060503. https://doi.org/10.1117/1.AP.5.6.060503
Lima CN et al (2022) Mannose-binding lectin conjugated to quantum dots as fluorescent nanotools for carbohydrate tracing. Methods Appl Fluoresc 10:025002. https://doi.org/10.1088/2050-6120/ac4e72
Lin B, Qing X, Liao J, Zhuo K (2020) Role of protein glycosylation in host-pathogen interaction. Cells 9:1022. https://doi.org/10.3390/cells9041022
Martínez-Alarcón D, Blanco-Labra A, García-Gasca T (2018) Expression of lectins in heterologous systems. Int J Mol Sci 19:616. https://doi.org/10.3390/ijms19020616
Mishra A et al (2019) Structure-function and application of plant lectins in disease biology and immunity. Food Chem Toxicol 134:110827. https://doi.org/10.1016/j.fct.2019.110827
Oliveira WF et al (2020a) Evaluating glucose and mannose profiles in Candida species using quantum dots conjugated with Cramoll lectin as fluorescent nanoprobes. Microbiol Res 230:126330. https://doi.org/10.1016/j.micres.2019.126330
Oliveira WF et al (2020b) Bauhinia monandra leaf lectin (BmoLL) conjugated with quantum dots as fluorescent nanoprobes for biological studies: application to red blood cells. Methods Appl Fluoresc 8:035009. https://doi.org/10.1088/2050-6120/ab9694
Oliveira WF et al (2022) Revealing glycobiology by quantum dots conjugated to lectins or "Borono-Lectins". In: Gopi S, Balakrishnan P, Mubarak NM (eds) Nanotechnology for biomedical applications. Springer, Singapore, pp 351–380. https://doi.org/10.1007/978-981-16-7483-9_16
Panniello A et al (2021) High-efficiency FRET processes in BODIPY-functionalized quantum dot architectures. Chem A Eur J 27:2371–2380. https://doi.org/10.1002/chem.202003574

Park YJ et al (2020) Role of CdSe and CdSe@ZnS quantum dots interlayers conjugated in inverted polymer solar cells. Org Electron 82:105707. https://doi.org/10.1016/j.orgel.2020.105707

Pereira G et al (2019) (Bio)conjugation strategies applied to fluorescent semiconductor quantum dots. J Braz Chem Soc 30: 2536–2561. https://doi.org/10.21577/0103-5053.20190163

Pessoa RBG et al (2019) The genus Aeromonas: a general approach. Microb Pathog 130:81–94. https://doi.org/10.1016/j.micpath.2019.02.036

Pessoa RBG et al (2022) Aeromonas and human health disorders: clinical approaches. Front Microbiol 13:868890. https://doi.org/10.3389/fmicb.2022.868890

Pessoa RBG et al (2023) Fluorescent nanoprobes based on quantum dots conjugated to Cramoll to assess surface carbohydrates of Aeromonas spp. Biochim Biophys Acta (BBA) Gen Subj 1867:130373. https://doi.org/10.1016/j.bbagen.2023.130373

Pinho SS et al (2023) Immune regulatory networks coordinated by glycans and glycan-binding proteins in autoimmunity and infection. Cell Mol Immunol 20:1101–1113. https://doi.org/10.1038/s41423-023-01074-1

Ramalingam G et al (2020) Quantum confinement effect of 2D nanomaterials. In: Divsar F (ed) Quantum dots - fundamental and applications. IntechOpen, London, pp 11–21. https://doi.org/10.5772/intechopen.90140

Ramírez-Herrera DE et al (2019) CdTe quantum dots modified with cysteamine: a new efficient nanosensor for the determination of folic acid. Sensors 19:4548. https://doi.org/10.3390/s19204548

Rathee G et al (2025) Quantum dots@layered double hydroxides: emerging nanocomposites for multifaceted applications. Prog Mater Sci 150:101403. https://doi.org/10.1016/j.pmatsci.2024.101403

Reynolds M, Pérez S (2011) Thermodynamics and chemical characterization of protein-carbohydrate interactions: the Multivalency Issue. C R Chim 14:74–95. https://doi.org/10.1016/j.crci.2010.05.020

Riu F et al (2022) Antibiotics and carbohydrate-containing drugs targeting bacterial cell envelopes: an overview. Pharmaceuticals 15:942. https://doi.org/10.3390/ph15080942

Sahu A, Kumar D (2022) Core-shell quantum dots: a review on classification, materials, application, and theoretical modeling. J Alloy Compd 924:166508. https://doi.org/10.1016/j.jallcom.2022.166508

Sanmartín-Matalobos J et al (2022) Semiconductor quantum dots as target analytes: properties, surface chemistry and detection. Nanomaterials 12:2501. https://doi.org/10.3390/nano12142501

Silva AR et al (2021a) Quantum dots conjugated to lectins from Schinus terebinthifolia leaves (SteLL) and Punica granatum sarcotesta (PgTeL) as potential fluorescent nanotools for investigating Cryptococcus neoformans. Int J Biol Macromol 192:232–240. https://doi.org/10.1016/j.ijbiomac.2021.10.002

Silva SP et al (2021b) Purification, characterization, and assessment of antimicrobial activity and toxicity of Portulaca elatior leaf lectin (PeLL). Probiotics Antimicrob Proteins 15:287–299. https://doi.org/10.1007/s12602-021-09837-w

Silva PM et al (2024) Punica granatum sarcotesta lectin (PgTeL) inhibits Pseudomonas aeruginosa replication, viability, aggregation, and biofilms. S Afr J Bot 165:264–274. https://doi.org/10.1016/j.sajb.2023.12.040

Sowers KL et al (2016) Photophysical properties of CdSe/CdS core/shell quantum dots with tunable surface composition. Chem Phys 471:24–31. https://doi.org/10.1016/j.chemphys.2015.09.010

Szymanski CM (2022) Bacterial glycosylation, it's complicated. Front Mol Biosci 9:1015771. https://doi.org/10.3389/fmolb.2022.1015771

Tenório DPLA et al (2015) CdTe quantum dots conjugated to concanavalin A as potential fluorescent molecular probes for saccharides detection in Candida albicans. J Photochem Photobiol B 142:237–243. https://doi.org/10.1016/j.jphotobiol.2014.11.010

Tobola F, Wiltschi B (2022) One, two, many: strategies to alter the number of carbohydrate binding sites of lectins. Biotechnol Adv 60:108020. https://doi.org/10.1016/j.biotechadv.2022.108020

Tsaneva M, Van Damme EJM (2020) 130 years of plant lectin research. Glycoconj J 37:533–551. https://doi.org/10.1007/s10719-020-09942-y

Turner MW (2003) The role of mannose-binding lectin in health and disease. Mol Immunol 40:423–429. https://doi.org/10.1016/S0161-5890(03)00155-X

Utama GL et al (2023) Potential application of yeast cell wall biopolymers as probiotic encapsulants. Polymers (Basel) 15:3481. https://doi.org/10.3390/polym15163481

Vasudevan D et al (2021) Core–shell quantum dots: properties and applications. J Alloy Compd 636:395–404. https://doi.org/10.1016/j.jallcom.2015.02.102

Vo NT et al (2016) Stability investigation of ligand-exchanged CdSe/ZnS-Y (Y =3-mercaptopropionic acid or mercaptosuccinic acid) through zeta potential measurements. J Nanomater 8564648. https://doi.org/10.1155/2016/8564648

World Health Organization (2022) Fungal priority pathogens list to guide research, development and public health action. World Health Organization Web. https://www.who.int/publications/i/item/9789240060241. Accessed 26 Nov 2024

Yao J et al (2017) Quantum dots: from fluorescence to chemiluminescence, bioluminescence, electrochemiluminescence, and electrochemistry. Nanoscale 9:13364–13383. https://doi.org/10.1039/c7nr05233b

Yazer M, Olsson M, Palcic M (2006) The cis-AB blood group phenotype: fundamental lessons in glycobiology. Transfus Med Rev 20:207–217. https://doi.org/10.1016/j.tmrv.2006.03.002